EasyChair Preprint

№ 9333

fNIRS-Based Command Generation to Control Robotic Hand Gripping

Jamila Akhter, Noman Naseer and Hammad Nazeer

November 17, 2022

fNIRS-based Command Generation to Control Robotic Hand Gripping

Jamila Akhter
Air University Islamabad, Pakistan
jamila.akhter@mail.au.edu.pk

Noman Naseer
Air University Islamabad, Pakistan
noman.naseer@mail.au.edu.pk

Hammad Nazeer Gilani
Air University Islamabad, Pakistan
Hammad@mail.au.edu.pk

***Abstract*—** Command generation to control robotic hand gripping is a demanding application of brain-computer interfacing (BCI) in automotive manufacturing, rehabilitation, and service robots. In this experimental work, the functional Near InfraRed Spectroscopy (fNIRS) based command is generated to control robotic hand gripping. Commands generated with improved accuracy of machine learning classifiers using acquired data from motor area of brain cortex. Results show 98% reliable performance of robot hand grasping and releasing of objects with a variety of shapes and surface characteristics within the workspace. In the future, generated commands can be applied in real-time automotive manufacturing robot control.

Keywords—functional Near Infrared Spectroscopy (fNIRS), robot hand gripping, machine learning classifiers

Introduction

The BCI is a unidirectional and occasionally bidirectional interaction concerning the living brain and peripheral devices such as computers, which excludes human muscle activation. BCI technology provides rehabilitation to patients with motor impairments and enhancement in the working ability of humans either cognitively or physically [1]. In controlling devices and the environment through BCI applications, the most challenging factor is the complexity of the human brain. The human brain is an extremely complicated dynamical system in accordance with nonlinear dynamics, comprising about 86 billion neurons [2]. The nerve cells are linked together by synapses to create a complicated network where connection is represented by synapses and neurons, as given in figure 1. To know the current status of the brain neural networks and dynamics of different brain areas time-spatial features are captured via placing sensors either on the scalp or within the cerebral cortex. Depicted features provide valuable information to control the amputee's prosthetic limbs [3] to enhance the excellence of post-stroke and post-traumatic patients' life by applying BCI technology. It offers extensive freedom both by improving or replacing human working ability and has applications in several fields such as robotics, physiotherapy, gate rehabilitation [4], gaming, and neuroscience[5].

Initially, BCI intention was to develop assistive and rehabilitative devices as biomedical applications[6]. But with the passage of time BCI technology significantly extended its applications in drowsiness detection to improve human performance at work [7] [8], approximating response time [9], brain-related fingerprinting lie detection system [10], virtual reality controlling [11], humanoid robots controlling [12] [13], quadcopters controlling in 3D space [14]and, BCI video games [15].

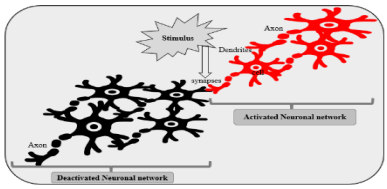

Figure 1: Activation and deactivation of nerve cell

BCI system shown in figure 2, includes brain signal recording, preprocessing of signals to remove physiological and experimental artifacts, selecting high signal-to-noise ratio channels, features extraction, signal classification, and an application of classified signals to control exoskeletons and robotic devices. [16] [17]

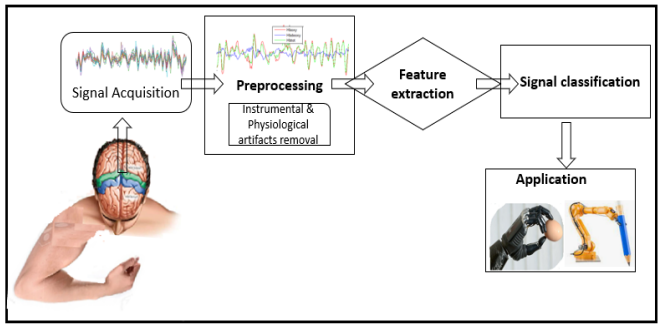

Figure 2: BCI system to control robotic hand gripping.

To record brain signals available imaging technologies are Electroencephalography (EEG), fNIRS and functional Magnetic Resonance Imaging (fMRI)[18]. Over the last decade, *f*NIRS has gained lots of attention as a non-invasive, portable, low-cost, and safe, functional neurological imaging technology to monitor brain activation during a particular activity[19].

fNIRS technology alternates with EEG and fMRI as it has limited penetration into the biological brain tissue, lower spatial resolution (2 to 3 cm), better sensitivity to superficial physiological motion artifacts, and noise, and resistance to motor artifacts. The fNIRS technology uses light optical proprieties in the wavelength of range 600 to 1000 nm (infrared light) to estimate regional hemodynamic responses (i.e., consumption of oxygen and increase in blood flow) in the active cortical area. Hemodynamic response changes are measured by the tissue optical absorption represented as signal contrast for oxygenated and deoxygenated hemoglobin in the fNIRS. Source-to-detector pairs, placed on the scalp at a distance of 3cm between each pair used to measure hemodynamic response [20], which is measured through changes in concentration of optical absorber, called chromophore (i.e., HbO and HbR, water, fats, etc.). In the brain tissue, each of chromophore has an explicit extinction or absorption coefficient, thus the influence of each chromophore molecule can be measured and can quantify its concentration level. The most common tissue chromophore is oxygen-dependent, called hemoglobin. Changes that occur in oxy-genated [HbO] and deoxy-genated [HbR] hemoglobin concentrations through activation and deactivation of the brain tissues are non-invasively measured in real-time using the NIRS technique [21]. To calculate deviation in [HbO] and [HbR], which are features of classifying the motor activity signals, Modified Beer-Lambert law is used [22]. Further, these classified signals are used for the amputees' prosthetic arm and robot control application.

Preceding findings on techniques for signal acquisition and classification approaches show encouraging results, but the best possible results are required for rehabilitation applications. In Sumit Raurale et al. [23] a Myo-Armband with 8 active surface EMG sensors was used for EMG-based hand-gripping brain signals acquisition for rehabilitation application with an accuracy of 95%. In Gene Shuman et al. [24] motor actions of the hand gripping and resting data were collected for 25-class problems using an accelerometer which shows an accuracy of 85%. ML classifier accuracies for the fNIRS-based data can be improved by data filtration and feature selection methods. In accordance with previous studies, fNIRS data filtration using Gaussian, Kalman, Butterworth, hemodynamic response filter (hrf), finite impulse response, and Wiener, has improved accuracies up to 97% [25]. Similarly, data filtration methods for feature selection are suggested such as genetic algorithms (GA) techniques for dimensionality reduction of the complex dimensional features [26], and the Z-score method for the channel's selection with 88.5% accuracies of ML classifiers [27].

In Haroon Khan et al. [28] six classes of motor activity of finger movements were investigated using eight different classifiers. The features selected from fNIRS -based ΔHbO data were signal mean, Skewness, Kurtosis, peak, minimum, variance, median, and peak-to-peak than 60% accuracies were observed with Neural Networking (NN), Support Vector Machine (SVM), AdaBoost, Linear Discriminant Analysis(LDA) and Decision Tree (DT) algorithms for classification problem. K-Nearest Neighbours (KNN), Random Forest, and XGBoost algorithms show accuracies of up to 77%. In Mustafa A. H. Hasan et al. [29] EEG, fNIRS, and hybrid EEG-fNIRS modalities were used to acquire motor task signals and their classification. For the classification of motor activity accuracy of 94.2% was achieved through the EEG-fNIRS hybrid, higher than that through EEG at 85.4% and fNIR at 92.4%.

The proposed study consists of two major parts. The first part consists of fNIRS data acquisition and the second part consist of features extraction, and feature classification to generate the command for robotics hand gripping control. In the second part by using the first part's results robotic arm controlling was done to grip the pen in the right hand and to grip other objects like eggs, glass, etc.

Materials and Methods

This session will describe the procedure followed during experimental design, data collection, pre-processing, and classification.

Participants

Ten healthy right-handed participants were chosen from the air university for hand-gripping data collection. The ages of the participants were 20–25 years. The enclosure criterion for right-handed participant selection was that they perform their daily activities with their right hand and no neurological disorders and motor disabilities were reported in their medical history. Literature review shows the best region to acquire motor activity is the primary motor cortex (M1) area of the brain: hand-gripping activity data acquired from the left as well as right hemispheres [30] [31] [32].

A verbal agreement was taken and participants were given instructions before conducting the experiment also Air University's Human Research Ethics Committee (HREC) has permitted the collection of data from university students. The trials were accomplished as per the ethical standards, allotted by the pronouncement of Helsinki [33].

Instrumentation and Optode Placement

fNIRS setup with aurora software used to acquire data under the supervision of the head of the mechatronics and biomedical department and research group at Air University Islamabad. The data collection was done, using 8 x 8 sensors array placed on the scalp surface onto the motor cortex area of the human. 10–20 system that creates 20 channels was used to acquire signals, 10 channels were created on right hemisphere and 10 channels on the left hemisphere. fNIRS optodes placement is shown in figure 3 a standard distance of 3 cm between the source and detector [34] [35]. Data collection was done with 760nm and 850nm IR wavelengths, i.e., at 10.1725 Hz sampling rate.

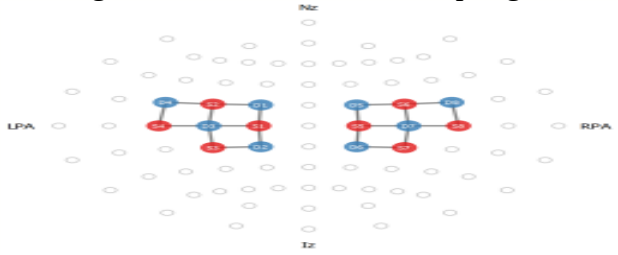

Figure 3: Optodes placement. Red color dots are sources and blue are detectors. Lines between sources and detectors represent channels.

Experimental paradigm

Experimental data was collected in a quiet and comfortable room. participants were given instructions to prevent the motion of their heads and unnecessary body movements. Initially, in paradigm there was 30s rest to generate a baseline, followed by an activity and rest cycle (10s activity and 10s rest) of 10 trials and informed by an alarm beep to start and stop the activity. An experimental paradigm of study is labeled in figure 4. Ignoring 60s rest at start and end of the experiment, individual experiment length was 200 s.

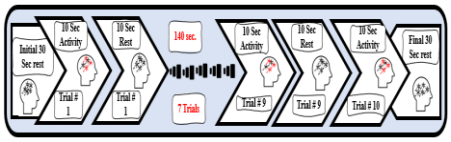

Figure 4: Experimental paradigm

The signal acquisition, processing, and feature extraction from oxy-and deoxyhemoglobin concentration data. Optical imaging techniques used in fNIRS to acquire hand gripping data 760nm and 850 nm wavelength of light intensity values were used [36].

The attained light intensities were processed using nirslab to eliminate undesirable data and gaps grabbed during the signal acquisition experiment. The data filtration and hemodynamic concentration are also computed with the same application.

Signal acquisition

The fNIRS setup provided with flexible cap and optodes placement marks on its' fabric. To acquire hand griping motor activity optodes were positioned on the surface of the scalp at the motor cortex area and the aurora software, based on MBLL was used. It converts the unprocessed signals to oxyhemoglobin and deoxyhemoglobin, by calculating the hemodynamic response. After wearing a cap with sensors and detectors on the head, optodes were calibrated. The connection between sensors and detector represents the channels. 20 channels were created and acquired raw data from all channels of subject 10 is shown in figure 5.

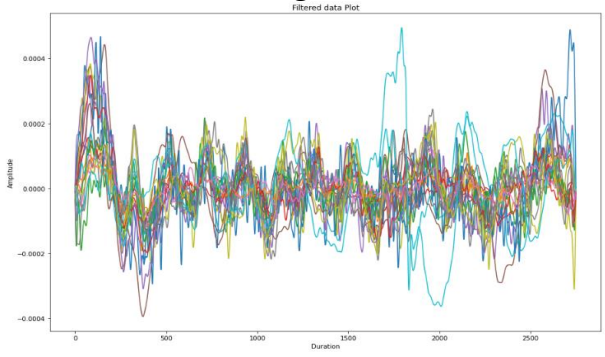

Figure 5: Raw signals acquired from fNIRS setup.

Signal processing

To attain maximum accuracy, data filtration and pre-processing were done using nirsLAB. The

physiological (0.5 Hz respiration, 1-1.5 Hz heartbeat, and blood pressure), and instrumental artifacts were eliminated through low pass filter with a cutoff frequency of 0.5 Hz and a 0.01 Hz cutoff frequency high-pass filter according to the literature review. By applying a bandpass filter resultant signal of multi-hemo state, oxyhemoglobin, deoxyhemoglobin, total hemoglobin, and oxygen saturation of channel 1 for subject 1 are shown in figure 6.

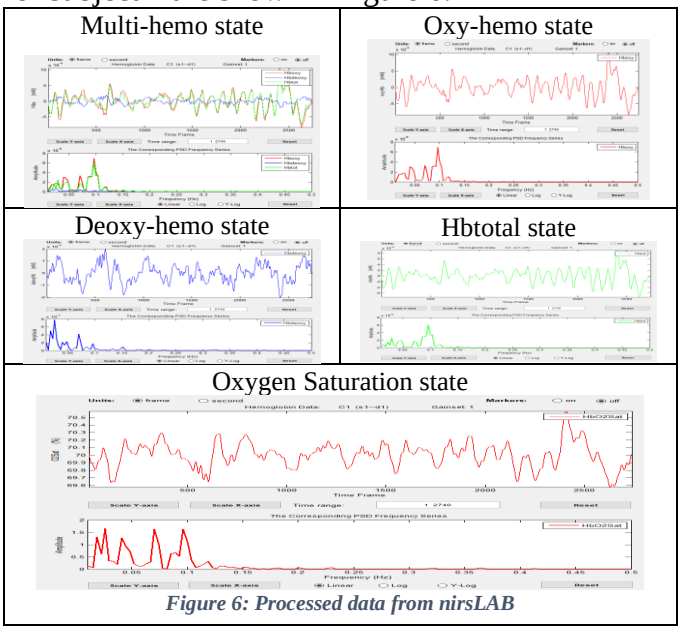

Figure 6: Processed data from nirsLAB

Feature Extraction

To improve the classifier accuracy for the hand gripping data the most common descriptive and morphological features extracted from filtered data are standard deviation, mean, Mean Absolute Deviation, maximum, minimum, signal entropy, and Interquartile range (IQR) (projection on a normally distributed density). Besides these statistical features data scaling features were also used to improve the classifier accuracy. Scaling features used are StandardScaler, RobustScaler, Quantile Transformation, Data discretization, PCA, and TruncatedSVD.

Classifiers

The machine learning classifier for the classification of the hand-gripping data used are LDA, Logistic Regression (LR), KNN, Decision Tree (DT), SVM and Naïve Bayes (NB).

Results

The results of this study comprise the classifier accuracies for the fNIRS-based hand-gripping data. Classifiers accuracies are given in table 2. The classification accuracy of the data without feature extraction was observed given in table 2 and the highest accuracy observed using six classifiers is of the KNN and DT represented in Figure 7a.

In order to improve the classifier accuracies, the scaling method was used as a feature and the result is shown in table 2 with a plot in figure 7b with improved accuracies of classifiers. Classifiers show up to 98% accuracy for deoxyhemoglobin concentration. The statistical features were also extracted from preprocessed data, plotted in figure 7b, showing no improvement in classifier accuracies.

In figure 7b comparative results are also shown for classifiers' accuracies for preprocessed data, scaling features, and statistical features.

Subject-wise classification results were analyzed to calculate the average accuracy of all subject's data. The noisy signals resulting in error were refined by repetition of pre-processing steps.

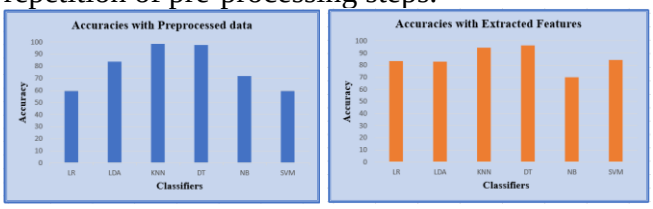

Figure 7 a: Accuracies with Preprocessed Data and Scaling Features.

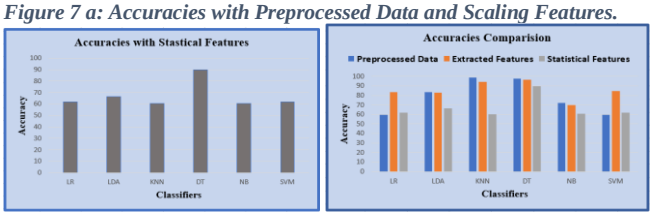

Figure 7 b: Statistical Features and other Accuracies Comparisons

Table 1: Classifiers accuracies for preprocessed data, scaling feature, and statistical features.

		Sub.1	Sub.2	Sub.3	Sub.4	Sub.5	Sub.6	Sub.7	Sub.8	Sub.9	Sub. 10	Average results
Raw Data Resul	**LR**	59.70	60.39	59.60	58.13	58.47	60.08	61.17	60.06	59.60	60.50	59.77
	LDA	87.59	78.75	89.98	86.93	87.12	85.20	77.52	82.96	74.05	86.89	83.69
	KNN	98.74	98.37	99.06	97.92	98.82	98.71	99.11	98.70	97.63	98.62	98.56

	DT	97.11	96.93	98.59	97.37	98.13	97.62	98.29	97.38	96.88	97.08	97.53
	NB	81.39	63.91	75.42	69.25	78.58	68.54	58.91	70.27	69.67	83.85	71.98
	SVM	59.70	60.39	59.60	58.13	58.47	60.08	61.17	60.06	59.60	60.50	59.77
Statistical Features Results	**LR**	59.20	82.74	93.04	87.37	89.99	89.40	79.94	84.98	76.13	90.36	83.32
	LDA	59.21	82.14	91.23	87.82	88.73	88.50	80.43	84.75	75.63	89.27	82.77
	KNN	55.47	98.44	98.53	98.38	98.79	98.56	98.71	98.77	98.86	98.68	94.32
	DT	86.93	97.07	98.32	97.07	98.43	97.43	98.26	97.56	96.15	97.73	96.49
	NB	59.53	63.72	75.70	69.77	79.43	70.42	56.60	69.80	68.77	84.35	69.8
	SVM	59.20	83.23	94.49	88.52	91.10	90.18	81.58	86.75	77.45	91.14	84.36
Feature data Results	**LR**	91.94	58.89	58.37	56.90	57.11	58.86	60.17	58.56	58.37	58.61	61.78
	LDA	89.96	60.62	72.32	64.40	62.02	67.54	61.03	59.34	65.18	62.09	66.45
	KNN	98.55	57.49	55.63	51.81	57.85	58.07	58.54	54.11	56.78	55.14	60.34
	DT	97.61	89.72	93.11	82.97	92.94	88.92	94.96	89.50	79.53	90.30	89.95
	NB	81.70	59.44	60.67	62.05	50.99	58.61	54.26	61.87	59.86	57.73	60.71
	SVM	92.85	58.89	58.37	56.90	57.11	58.86	60.17	58.56	58.37	58.91	61.89

Conclusion

In this research study, hand-gripping data was recorded using an fNIRS-based approach. Brain signals from the motor cortex region are acquired. nirsLAB software with bandpass filters was applied to filter the physiological, motion, and instrumental artifacts. The statistical features set to improve classifier accuracies were SD, mean, mean absolute deviation, minimum, signal entropy, and interquartile range (IQR) but no reasonable accuracy improvements were observed. The scaling features were also used with valuable increments in classifiers' accuracies. LR, LDA, KNN, DT, SVM, and NB classifiers were used to achieve maximal accuracy. The highest accuracy with individual subject data was noted as 98%. In the future, the presented work can be possibly extended for accuracy enhancement using deep learning neural networks along with more hand gestures to control the 3D motion of the robotic arm. Controlling robotic arm motions by the implementation of generated commands in real time is another focus for future work.

References

[1] S. Saha et al., "Progress in Brain Computer Interface: Challenges and Opportunities," Frontiers in Systems Neuroscience, vol. 15. Frontiers Media S.A., Feb. 25, 2021. doi: 10.3389/fnsys.2021.578875.

[2] S. Herculano-Houzel, "The human brain in numbers: A linearly scaled-up primate brain," Frontiers in Human Neuroscience, vol. 3, no. NOV. Frontiers Media S. A., Nov. 09, 2009. doi: 10.3389/neuro.09.031.2009.

[3] S. Saha et al., "Progress in Brain Computer Interface: Challenges and Opportunities," Frontiers in Systems Neuroscience, vol. 15. Frontiers Media S.A., Feb. 25, 2021. doi: 10.3389/fnsys.2021.578875.

[4] Khan, R., Naseer, N., Nazeer, H., & Khan, M. N. (2018). Control of a prosthetic leg based on walking intentions for gait rehabilitation: an fNIRS study. Frontiers in Human Neuroscience, 12.

[5] S. N. Abdulkader, A. Atia, and M. S. M. Mostafa, "Brain computer interfacing: Applications and challenges," Egyptian Informatics Journal, vol. 16, no. 2. Elsevier B.V., pp. 213–230, Jul. 01, 2015. doi: 10.1016/j.eij.2015.06.002.

[6] V. A. Maksimenko et al., "Neural Interactions in a Spatially-Distributed Cortical Network During Perceptual Decision-Making," Frontiers in Behavioral Neuroscience, vol. 13, Sep. 2019, doi: 10.3389/fnbeh.2019.00220.

[7] C. S. Wei, Y. te Wang, C. T. Lin, and T. P. Jung, "Toward Drowsiness Detection Using Non-hair-Bearing EEG-Based Brain-Computer Interfaces," IEEE Transactions on Neural Systems and Rehabilitation Engineering, vol. 26, no. 2, pp. 400–406, Feb. 2018, doi: 10.1109/TNSRE.2018.2790359.

[8] J. Too, A. R. Abdullah, N. M. Saad, and W. Tee, "EMG feature selection and classification using a Pbest-guide binary particle swarm optimization," Computation, vol. 7, no. 1, 2019, doi: 10.3390/computation7010012.

[9] P. Aricò et al., "Adaptive automation triggered by EEG-based mental workload index: A passive brain-computer interface application in realistic air traffic control environment," Frontiers in Human Neuroscience, vol. 10, no. OCT2016, Oct. 2016, doi: 10.3389/fnhum.2016.00539.

[10] L. A. Farwell, D. C. Richardson, G. M. Richardson, and J. J. Furedy, "Brain fingerprinting classification concealed information test detects US Navy military medical information with P300," Frontiers in Neuroscience, vol. 8, no. DEC 2014, doi: 10.3389/fnins.2014.00410.

[11] J. M. Juliano et al., "Embodiment is related to better performance on a brain–computer interface in immersive virtual reality: A pilot study," Sensors (Switzerland), vol. 20, no. 4, Feb. 2020, doi: 10.3390/s20041204.

[12] B. Choi and S. Jo, "A Low-Cost EEG System-Based Hybrid Brain-Computer Interface for Humanoid Robot Navigation and Recognition," PLoS ONE, vol. 8, no. 9, Sep. 2013, doi: 10.1371/journal.pone.0074583.

[13] R. Spataro et al., “Reaching and grasping a glass of water by locked-In ALS patients through a BCI-controlled humanoid robot,” Frontiers in Human Neuroscience, vol. 11, Mar. 2017, doi: 10.3389/fnhum.2017.00068.
[14] K. Lafleur, K. Cassady, A. Doud, K. Shades, E. Rogin, and B. He, “Quadcopter control in three-dimensional space using a noninvasive motor imagery-based brain-computer interface,” Journal of Neural Engineering, vol. 10, no. 4, Aug. 2013, doi: 10.1088/1741-2560/10/4/046003.
[15] A. K. Singh, Y. K. Wang, J. T. King, and C. T. Lin, “Extended interaction with a bci video game changes resting-state brain activity,” IEEE Transactions on Cognitive and Developmental Systems, vol. 12, no. 4, pp. 809–823, Dec. 2020, doi: 10.1109/TCDS.2020.2985102.
[16] R. A. Khan, N. Naseer, N. K. Qureshi, F. M. Noori, H. Nazeer, and M. U. Khan, “FNIRS-based Neurorobotic Interface for gait rehabilitation,” Journal of NeuroEngineering and Rehabilitation, vol. 15, no. 1, Feb. 2018, doi: 10.1186/s12984-018-0346-2.
[17] N. Naseer and K. S. Hong, “fNIRS-based brain-computer interfaces: A review,” Frontiers in Human Neuroscience, vol. 9, no. JAN. Frontiers Media S. A., Jan. 28, 2015. doi: 10.3389/fnhum.2015.00003.
[18] M. A. H. Hasan, M. U. Khan, and D. Mishra, “A Computationally Efficient Method for Hybrid EEG-fNIRS BCI Based on the Pearson Correlation,” BioMed Research International, vol. 2020, 2020, doi: 10.1155/2020/1838140.
[19] S. M. R. Guérin, M. A. Vincent, C. I. Karageorghis, and Y. N. Delevoye-Turrell, “Effects of Motor Tempo on Frontal Brain Activity: An fNIRS Study,” Neuroimage, vol. 230, Apr. 2021, doi: 10.1016/j.neuroimage.2020.117597.
[20] T. J. Huppert, “Commentary on the statistical properties of noise and its implication on general linear models in functional near-infrared spectroscopy,” Neurophotonics, vol. 3, no. 1, p. 010401, Mar. 2016, doi: 10.1117/1.nph.3.1.010401.
[21] D. Grosenick, H. Rinneberg, R. Cubeddu, and P. Taroni, “Review of optical breast imaging and spectroscopy,” Journal of Biomedical Optics, vol. 21, no. 9, p. 091311, Jul. 2016, doi: 10.1117/1.jbo.21.9.091311.
[22] H. Abitan, H. Bohr, and P. Buchhave, “Correction to the Beer-Lambert-Bouguer law for optical absorption,” 2008.
[23] IEEE Signal Processing Society, 2018 IEEE International Conference on Acoustics, Speech and Signal Processing : proceedings : April 15-20, 2018, Calgary Telus Convention Center, Calgary, Alberta, Canada.
[24] G. Shuman, Z. Durić, D. Barbará, J. Lin, and L. H. Gerber, “Improving the recognition of grips and movements of the hand using myoelectric signals,” BMC Medical Informatics and Decision Making, vol. 16, Jul. 2016, doi: 10.1186/s12911-016-0308-1.
[25] Khan, R. A., Naseer, N., Saleem, S., Qureshi, N. K., Noori, F. M., & Khan, M. J. (2020). Cortical tasks-based optimal filter selection: an fNIRS study. Journal of Healthcare Engineering, 2020.
[26] F. M. Noori, N. K. Qureshi, R. A. Khan and N. Naseer, "Feature selection based on modified genetic algorithm for optimization of functional near-infrared spectroscopy (fNIRS) signals for BCI," *2016 2nd International Conference on Robotics and Artificial Intelligence (ICRAI)*, 2016, pp. 50-53, doi: 10.1109/ICRAI.2016.7791227.
[27] Nazeer, H., Naseer, N., Mehboob, A., Khan, M. J., Khan, R. A., Khan, U. S., & Ayaz, Y. (2020). Enhancing classification performance of fNIRS-BCI by identifying cortically active channels using the z-score method. Sensors, 20(23), 6995.].
[28] H. Khan, F. M. Noori, A. Yazidi, M. Z. Uddin, M. N. Afzal Khan, and P. Mirtaheri, “Classification of individual finger movements from right hand using fnirs signals,” Sensors, vol. 21, no. 23, Dec. 2021, doi: 10.3390/s21237943.
[29] M. A. H. Hasan, M. U. Khan, and D. Mishra, “A Computationally Efficient Method for Hybrid EEG-fNIRS BCI Based on the Pearson Correlation,” BioMed Research International, vol. 2020, 2020, doi: 10.1155/2020/1838140.
[30] I. Miyai et al., “Cortical mapping of gait in humans: A near-infrared spectroscopic topography study,” Neuroimage, vol. 14, no. 5, pp. 1186–1192, 2001, doi: 10.1006/nimg.2001.0905.
[31] S. L. Jacques, “Erratum: Optical properties of biological tissues: A review (Physics in Medicine and Biology (2013) 58),” Physics in Medicine and Biology, vol. 58, no. 14. pp. 5007–5008, Jul. 21, 2013. doi: 10.1088/0031-9155/58/14/5007.
[32] M. Mihara, I. Miyai, M. Hatakenaka, K. Kubota, and S. Sakoda, “Role of the prefrontal cortex in human balance control,” Neuroimage, vol. 43, no. 2, pp. 329–336, Nov. 2008, doi: 10.1016/j.neuroimage.2008.07.029.
[33] S. Lloyd-Fox, A. Blasi, and C. E. Elwell, “Illuminating the developing brain: The past, present and future of functional near infrared spectroscopy,” Neuroscience and Biobehavioral Reviews, vol. 34, no. 3. pp. 269–284, Feb. 2010. doi: 10.1016/j.neubiorev.2009.07.008.
[34] M. Legrand, N. Jarrassé, F. Richer, and G. Morel, “A closed-loop and ergonomic control for prosthetic wrist rotation.”
[35] F. Herold, P. Wiegel, F. Scholkmann, A. Thiers, D. Hamacher, and L. Schega, “Functional near-infrared spectroscopy in movement science: a systematic review on cortical activity in postural and walking tasks,” Neurophotonics, vol. 4, no. 4, p. 041403, Aug. 2017, doi: 10.1117/1.nph.4.4.041403.
[36] N. Naseer, M. J. Hong, and K. S. Hong, “Online binary decision decoding using functional near-infrared spectroscopy for the development of brain-computer interface,” Experimental Brain Research, vol. 232, no. 2, pp. 555–564, Feb. 2014, doi: 10.1007/s00221-013-3764-1.